

Constant power control of variable speed wind farm for primary frequency control support

Sadegh Ghani Varzaneh¹ · Mehrdad Abedi¹ ·
G. B. Gharehpetian¹

Received: 25 December 2016 / Accepted: 20 October 2017 / Published online: 23 March 2018
© Springer-Verlag GmbH Germany, part of Springer Nature 2018

Abstract The increasing penetration level of wind energy conversion systems (WECSs) into power systems imposes new requirements on the contribution of WECSs in the frequency control system. These requirements can be fulfilled by modifying the conventional control system of WECS. However, special attention should be paid to the frequency response of WECS, which should be high enough to contribute to frequency control, but should not lead to instability of WECS. Since a wind farm contains many turbines, determining the optimal response is very difficult. In this paper, by coordinating the WECSs of a variable speed wind farm, a pre-scheduled power can be tracked. Therefore, the fluctuation of the output power is mitigated; an optimal frequency response is achieved and the stability of WECSs is guaranteed. Simulation results show the capability of the proposed scheme to enable the wind farm tracks a pre-scheduled power and improves frequency control.

Keywords Constant power control · Wind farm · Frequency control · Deloading · Droop control

✉ Sadegh Ghani Varzaneh
sadegh_ghani@aut.ac.ir; sadegh1366ghani@gmail.com

Mehrdad Abedi
abedi3@aut.ac.ir

G. B. Gharehpetian
grptian@aut.ac.ir

¹ Electrical Engineering Department, Amirkabir University of Technology (Tehran Polytechnic), No. 424, Hafez ave., Tehran 15914, Iran

1 Introduction

Due to economic and environmental issues, integration of wind energy conversion systems (WECSs) into power systems is rapidly increasing, which may negatively affect the stability of power system [1,2]. Especially, when the wind speed is high and power system operates in off-peak hours, this situation gets worse. Since variable speed WECSs employ power electronic interfaces, they do not have an intrinsic response to the frequency deviations [3]. The frequency deviations may lead to tripping of generators and sensitive loads, and therefore, the reliability of power system decreases.

In order to behave in the same way as the conventional power plant, the inertial and the droop controls can be added to the conventional control system of the WECS. During the inertial response, which lasts about 10 s [4,5], sufficient energy can be injected to (or absorbed from) the grid to reduce the rate of change of frequency. This energy can be supplied by the kinetic energy stored in the rotating mass of WECSs. The droop control, i.e., the primary frequency control, can be used for releasing the reserve power according to the frequency deviation. The primary frequency control should be activated within 15–23 s [6] and it minimizes the difference between load and generation [4,7]. The WECS should have sufficient generation reserve margin to be able to participate in this level of control. Therefore, during nominal frequency conditions, the WECS should operate in a suboptimal region, known as deloaded operation, to reserve sufficient power [2,8–10]. The loss of revenue, due to the operation in the suboptimal region, can be compensated by taking part in the frequency control market [4]. Furthermore, participation of WECSs in frequency control of electrical grids that do not have fast-ramping generators is very useful [11].

During the inertial control, the amount of the WECS injected power can be temporarily higher than the maximum power of the turbine and, therefore, the turbine rotational speed reduces. In case of continuous deceleration, the instability may occur. Some studies have been carried out to improve the inertial response and ensure the stability [12–15]. The present study does not focus on this level of control.

In the droop control scheme, as the droop value decreases, the amount of the injected power increases. However, if the droop value is set to a value lower than the critical one, the rotational speed of the WECS decreases and WECS becomes unstable [9]. This instability leads to a reduction in injected active power of WECS and, therefore, the frequency decreases. Moreover, due to wind speed variations, which cause the fluctuations in the WECS prime-mover, the instability is more likely and, therefore, a low droop value cannot be set. On the other hand, if the droop value is adjusted to a very high value, the additional injected power of WECS will be too small to contribute to frequency control and WECS will operate in a suboptimal condition. To guarantee stability, the droop value can vary according to the generation margin or wind speed [9,16,17]. However, estimating the generation margin is not an easy task and the scheme depends on the operating point of the WECS.

Another point of view is that due to variations of wind speed, the output power of WECS fluctuates. When the penetration of WF into the power system is increased, the fluctuations of the output power may cause problems. Especially, the problems get worse when the WF is connected to a weak grid. Not only the output power fluctuations may lead to frequency deviations [18,19], but also they may cause voltage

flicker, excessive line losses and instability problem [1, 20–22]. Furthermore, using the conventional power plant for the reduction of frequency variations, imposes additional costs and leads to wear of the generator [19].

In the present paper, the conventional controller of WECS is modified and a simple supervisory controller is introduced which coordinates the WECSs installed in a wind farm (WF). The contributions of the present paper are as follows:

- The proposed scheme guarantees the stability of turbines participating in the primary frequency control.
- In the proposed scheme, by adjusting a low droop constant, more wind power can be delivered during the primary frequency control.
- The scheme is very simple and does not depend on the turbine operating point.
- Also, it mitigates the complexity of providing the generation reserve margin.
- The proposed scheme can enable the WF to produce a constant power. Therefore, during the deloaded operation, the fluctuation of output power is significantly mitigated.

This paper is organized as follows; in the next section, modeling and control of WECS is introduced. The conventional inertial and droop controls are reviewed in Sect. 3. In Sect. 4, the proposed frequency control is introduced. Simulation results are presented in Sect. 5. The capabilities of the proposed scheme are discussed in Sect. 6. Finally, the conclusion is drawn in the last section.

2 Modeling and control of WECS

In a WECS, different types of generators can be employed. In order to get the maximum power, it is better to employ variable speed structures. Among these types of generators, the doubly fed induction generator (DFIG) is a good option. Due to the lower converter rating, the costs and the weight of the DFIG are lower in comparison with other types [23, 24]. Therefore, in this paper, it is assumed that the WF is equipped with this type of generator.

2.1 Wind turbine system

The turbine power P_m in Watt is as follows [6]:

$$P_m = \frac{1}{2} \rho A C_p v^3 \quad (1)$$

where ρ is the air density in $\frac{kg}{m^3}$, A is the swept area in m^2 , v is the wind speed in $\frac{m}{s}$ and C_p is the turbine aerodynamic efficiency obtained from $C_p(\lambda, \beta)$ curve. λ and β are the tip speed ratio (TSR) and pitch angle, respectively. The TSR is given as follows:

$$\lambda = \frac{R\omega_r}{v} \quad (2)$$

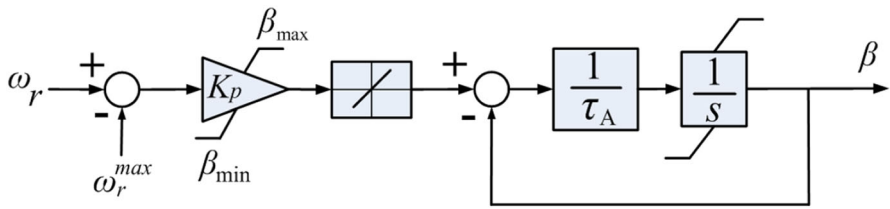


Fig. 1 The pitch angle control system

where R and ω_r are rotor radius in m and turbine rotational speed in rad/s, respectively. The curve of C_p used in this paper is as follows [6]:

$$C_p(\lambda, \beta) = 0.73 \left(\frac{151}{\lambda_i} - 0.58\beta - 0.002\beta^{2.14} - 13.2 \right) e^{-\frac{18.4}{\lambda_i}}$$

$$\lambda_i = \frac{1}{\frac{1}{\lambda - 0.2\beta} - \frac{0.003}{\beta^3 + 1}} \tag{3}$$

If the pitch angle is increased, C_p and turbine mechanical power reduce. Figure 1 shows the pitch angle control system [6]. For rotational speeds lower than the predetermined value (ω_r^{max}), the pitch angle is not varied and the capability of maximum power point tracking (MPPT) is achieved. However, for rotational speeds higher than ω_r^{max} , the pitch control system is activated to protect the WECS from over speeding and over loading.

2.2 Modeling of the drive train

We consider the lump mass model for the drive-train. The single equivalent mass shows the effect of the generator and the turbine inertia. The dynamic equation is expressed as follows [6]:

$$\frac{d\omega_r}{dt} = \frac{1}{2H} (T_m - T_e) \tag{4}$$

where H is the lumped inertia constant in s, T_m and T_e are the mechanical and electrical torques, respectively.

2.3 Control of the DFIG-based WECS

There are two controllers in a DFIG-based turbine named the rotor side converter (RSC) and the grid side converter (GSC) controllers. The active and reactive powers are adjusted by the RSC controller, while the GSC controller is responsible for regulating the DC-link voltage. In this paper, the control of the RSC will be discussed. Details about the GSC controller have been presented in [25].

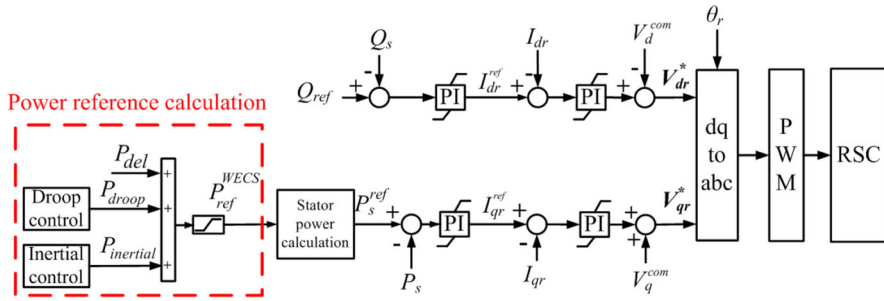


Fig. 2 The conventional vector control of the RSC

3 Participation of WECS in the frequency control system

The conventional control of the RSC is depicted in Fig. 2 [26]. The power reference of the WECS is determined based on the deloaded power, i.e., P_{del} , the inertial control, i.e., $P_{inertial}$, and the droop control, i.e., P_{droop} [7]. The power reference is tracked by the RSC controller. In the following subsections, the conventional deloaded operation of wind turbine, the conventional inertial and droop controls are reviewed.

3.1 Conventional deloaded operation of wind turbine

For any wind speed, there is a specific rotational speed at which the maximum power of the turbine (P_{opt}) can be obtained [27]. The maximum power of the turbine can be obtained, if the power reference of WECS is governed by the following equations [28]:

$$\begin{aligned}
 P_{opt} &= K_{opt} \omega_r^3 \\
 K_{opt} &= \frac{1}{2} \rho \pi R^5 \frac{C_p^{max}}{\lambda_{opt}^3}
 \end{aligned}
 \tag{5}$$

where λ_{opt} is the optimal value of the TSR and C_p^{max} is the maximum value of the aerodynamic efficiency of the turbine. As explained earlier, the WECSs should have sufficient power reserve margin to be able to take part in the primary frequency control. To deload a WECS, either the pitch control or the over speeding methods can be used to derivate C_p from its optimal value [4, 10]. The dynamic of the pitch angle control system is slow and frequent variation of the pitch blades would decrease the lifetime of the WECS [29]. Therefore, it is suggested to use the over speeding method under rated wind speed. As discussed in [5, 8, 9], if the reference power of an individual turbine (P_{ref}) is set according to the following equation, a specific generation reserve margin is obtained:

$$P_{ref} = P_{del} + (P_{opt} - P_{del}) \frac{\omega_r^{del} - \omega_r}{\omega_r^{del} - \omega_r^{opt}}
 \tag{6}$$

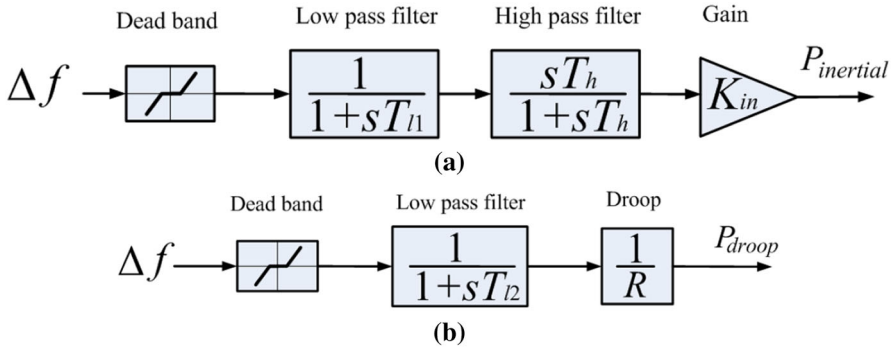


Fig. 3 The conventional frequency control: **a** the inertial control and **b** the droop control

where P_{del} and ω_r^{del} are the deloaded power and the generator rotational speed at P_{del} , respectively. By varying the wind speed, all variables of the above equation will change. Therefore, the implementation of this method is complicated and the error in the estimation of variables will result in the malfunction of the scheme. Furthermore, the conventional over speeding method imposes additional fluctuations on the output power [18]. In this paper, by coordinating WECSs in the WF, these challenges are resolved, since the proposed scheme does not rely on the operating point of turbines and the fluctuations of output power are significantly mitigated.

3.2 Conventional inertial control

Figure 3a shows the control diagram of the virtual inertia [7]. The frequency deviation is determined by the following equation:

$$\Delta f = f_{ref} - f_{meas} \quad (7)$$

where f_{ref} and f_{meas} are the reference and the measurement of the frequency, respectively. Firstly, by using the low pass filter, measurement noise is eliminated. To avoid the reaction of the controller to the small change in the frequency deviation, employing the dead band is essential. The high pass filter has two functions; it limits the response of the controller in the steady-state condition and also contributes to the recovery process of rotational speed [30]. Finally, K_{in} is employed to adjust the response of WECS.

3.3 Conventional droop control

The droop control responds to the steady-state frequency deviation. Figure 3b shows the block diagram of conventional droop control [7]. The dead band is used to prevent the reaction of the controller on small changes of the frequency deviation. Similar to the conventional governor, the droop value (i.e., R) is employed to specify the response of the WECS to the frequency deviation.

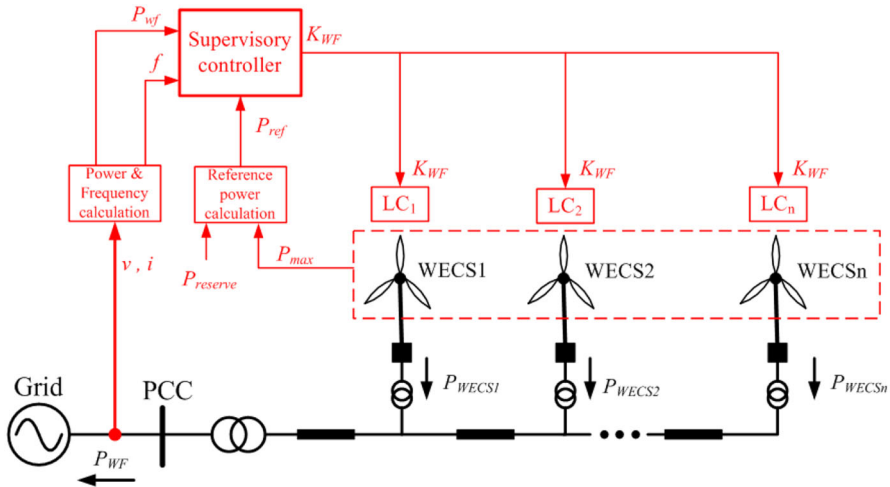


Fig. 4 The proposed scheme

It is clear that as the droop value decreases, electrical power increases. According to Eq. 4, if electrical power becomes higher than the maximum mechanical power, turbine decelerates. In case of continuous deceleration, instability may occur. Note that due to the wind speed variation, the mechanical power varies continuously, and the instability is more likely. To preserve the stability, electrical power should be kept lower than the maximum mechanical power in all conditions. Applying the high droop value results in decreasing electrical power and preserving the stability, but the WECS operates in a suboptimal region. During the primary frequency control, it is useful to inject the reserve power of the WECS as much as possible.

In the proposed scheme, by adjusting a low droop constant, more wind power can be delivered during the primary frequency control. Furthermore, the scheme guarantees the stability of turbines.

4 Proposed scheme

The proposed scheme aims to coordinate all turbines in a WF for two purposes. Firstly, during the deloaded operation, the complexity of providing a generation reserve margin is reduced and also fluctuations of output power are significantly reduced. Secondly, during the primary frequency control, the stability of turbines is guaranteed and also a low droop constant is adjusted to increase the delivered power of WF.

Figure 4 shows the proposed frequency control scheme which consists of two levels. At the first level, i.e., the local controller (LC), the conventional control of the WECS is changed while, at the second control level, a supervisory controller coordinates all WECSs based on different scenarios. The supervisory controller is very simple and does not depend on the WECSs operating points. But the maximum available power of WECSs (P_{max}) should be known.

4.1 The proposed local controller

In this study, the deloaded operation is achieved by adjusting the power reference of the WECS as follows:

$$\begin{aligned} P_{del} &= K_{del}\omega_r^3 \\ K_{del} &= \frac{1}{2}\rho\pi R^5 \frac{C_p^{del}}{\lambda_{del}^3} \end{aligned} \quad (8)$$

where λ_{del} and C_p^{del} are the TSR and aerodynamic efficiency of turbine operated in the deloaded state. The Eq. 8 can be rewritten as follows:

$$\begin{aligned} P_{del} &= K_{opt}\omega_r^3 - K_{WF}\omega_r^3 \\ K_{WF} &= K_{opt} - K_{del} \end{aligned} \quad (9)$$

According to Eqs. 8 and 9, the term $K_{WF}\omega_r^3$ is the amount of the reserve power. The value of K_{WF} is a determining factor in the deloading strategy of WECS. When K_{WF} is positive, the power reference of WECS, i.e., P_{del} , is lower than the maximum mechanical power, i.e., P_{opt} . Therefore, according to Eq. 4, the WECS accelerates and the deloaded operation is achieved. The acceleration of the turbine continues until the turbine power becomes equal to P_{del} .

When the wind speed is above the rated value, the rotational speed is limited by the pitch control system and the maximum power of turbine is 1 pu. Therefore, the power reference of the WECS is as follows:

$$P_{del} = 1 - K_{WF}\omega_r^3 \quad (10)$$

From 10, by increasing K_{WF} , the power reference decreases and, therefore, the rotational speed and the pitch angle increase. Increasing the pitch angle continues until the mechanical power becomes equal to P_{del} .

Figure 5 shows the proposed local controller of the WECS, which is based on Eq. 9. The lower and upper bounds of P_{opt} are 0 and 1 pu, respectively. The K_{WF} is simply determined by the supervisory controller. The K_{WF} is used to deload the WF in nominal frequency conditions and provides the droop control during frequency disturbances. Therefore, the conventional droop control is removed from the local controller and the complexity is reduced. The reference power is tracked by the RSC controller shown in Fig. 2.

In order to mitigate the mechanical stress on the turbine and generator, the rate of change of output power of WECS should be limited. The maximum rate of change of DFIG power is $0.45 \frac{pu}{s}$ [31]; therefore, the presence of a rate limiter is essential.

4.2 The proposed supervisory controller

The function of the supervisory controller is to specify K_{WF} and distribute it among local controllers. Details about the communication system of a WF have been presented

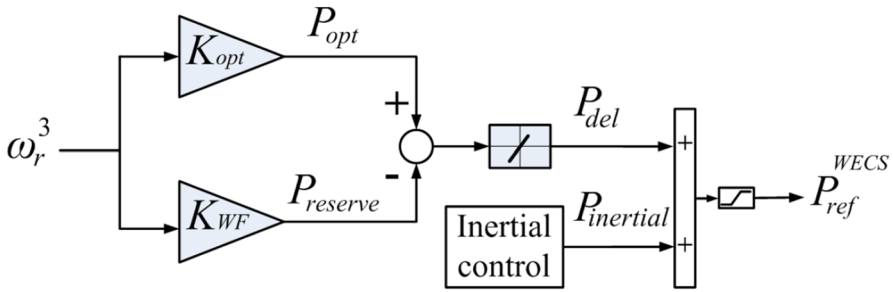


Fig. 5 The proposed local controller

in [32]. It should be noted that K_{WF} is positive and can be adjusted based on two different scenarios. In the first scenario, the supervisory controller can be used to enable the WF tracks a pre-scheduled power. In the second scenario, the supervisory controller provides a deloading control strategy in nominal frequency conditions. However, it provides the droop control strategy during frequency disturbances. Below explanation provides details of these scenarios.

By accelerating turbine, C_p deviates from the maximum value and turbine operates in the deloaded state. In this condition, the kinetic energy stored in the rotating mass of turbines, can be employed as an energy source to mitigate the fluctuations of the output power and produce a constant power. Figure 6a shows the first scenario of the supervisory controller. In this scenario, the pre-scheduled power, i.e., P_{ref} , is compared with the output power of the WF, i.e., P_{wf} , and the error is processed by the PI controller. The output of the controller, i.e., K_{WF} , is used in all the local controllers and as a result, the desired power is tracked. Assuming that the power of the WF is higher than the demand, as shown in Fig. 6a, the error has a positive value which results in an increase in K_{WF} . Consequently, according to Eq. 9, the output power of WECSs reduces. The increasing of K_{WF} continues until the desired power is satisfied.

It should be noted that, if the reference power becomes higher than the maximum available power of the WF, the output of the PI controller becomes zero (i.e., $K_{WF} = 0$) and, according to Eq. 9, the maximum available power of the WF is tracked. Therefore, the instability could not occur.

Figure 6b shows the second scenario. During nominal frequency conditions, a pre-determined power, i.e., P_{ref} , is tracked which is less than the maximum available power. However, during low frequency conditions, the reserve power is injected to the grid by means of the droop controller. In this condition, if the demand power, i.e., $P_{ref} + P_{droop}$, becomes higher than the available power of the WF, K_{WF} becomes zero and the maximum power of the WF is tracked. Thus, without any concern about the instability problem, a low droop value can be adjusted. As will be shown in the next section, by adjusting a low droop value, the optimal frequency response of WF is achieved.

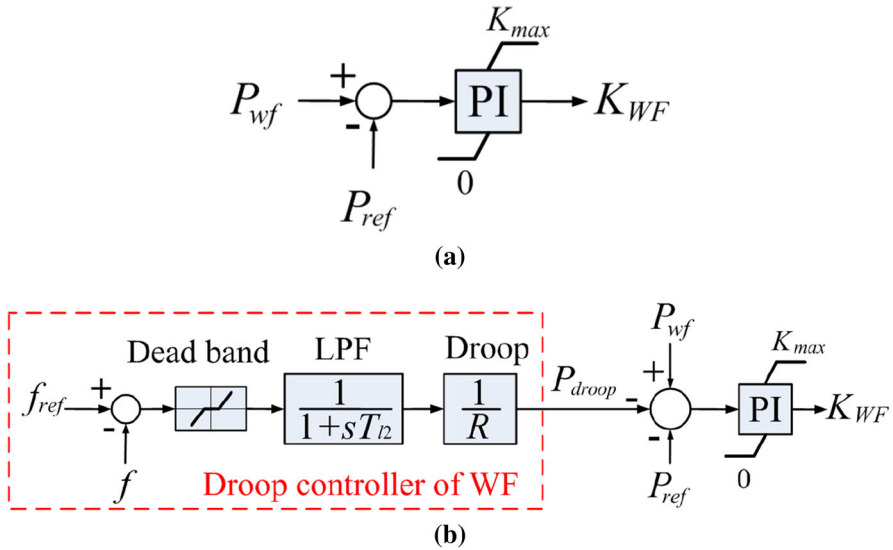


Fig. 6 The proposed supervisory controller: **a** constant power control strategy and **b** primary frequency control strategy

5 Case studies

5.1 Configuration of the power system under study

Figure 7 depicts the configuration of the power system under study. The conventional power plants consist of four hydro generators with the total capacity of 270 MW [33] ($G_1 = 120$ MW, $G_2 = 90$ MW, $G_3 = 30$ MW and $G_4 = 30$ MW) and the load is 165 MW with the damping constant of 2 pu. The inertia constant of the system is 4 s on 270 MVA base.

According to the grid code, the speed-droop characteristic of the conventional units can be set between 3 and 6% [9]. In this study, the droop setting of the conventional generators is 5%. More details about the conventional power plants are given in Appendix.

In order to study the comprehensive dynamic behavior of a WF, the WECSs should be separately simulated. In reference [34], an approach has been proposed to represent the entire WF with a limited number of WECSs. In the present study, as shown in Fig. 7, it is assumed that the WF contains 6 equivalent WECSs with nominal power of 60 MW. The simulation results have been carried out using MATLAB software with a realistic model of wind turbine described in [35]. The allowable upper and lower limits for the generator speed are 0.67 and 1.33 pu, respectively. Details about the parameters of the individual WECSs are given in Appendix.

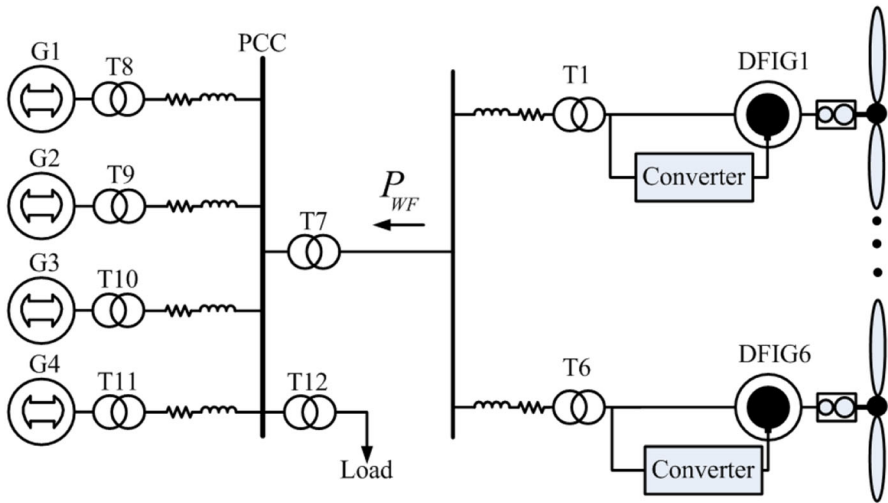


Fig. 7 The configuration of the power system under study

5.2 Reference active power tracking

In this section, the capability of constant power control strategy of the proposed scheme is investigated. As illustrated in Fig. 6a, the supervisory controller coordinates WECSs and, therefore, a pre-scheduled power can be tracked. In the first and second cases, the performance of the proposed scheme under constant wind speed is studied. In other cases, the wind speed variations are also taken into account.

In the first case, the performance of the proposed scheme in low wind speed condition is investigated. As it can be seen in Table 1, wind speed is lower than the rated value, i.e., $11.4 \frac{m}{s}$. If turbines operate in the MPPT mode, the output power of the WF is 30.5 MW. To obtain the demand of 25 MW, the output of the supervisory controller, i.e. K_{WF} , must be equal to 0.3 and it must be used in all local controllers. The pitch angle, the rotational speed and the output power of WECSs are also given in Table 1. Comparison between the deloaded and the MPPT modes shows that by accelerating turbines, the deloading strategy is achieved. Since the rotational speed of the fifth and sixth WECSs exceeds ω_r^{max} , i.e., 1.25 pu, the pitch control system is activated.

Table 2 shows the results of the second case study. The wind speeds of WECSs are higher than the rated value and, therefore, the pitch control system has been activated. To obtain the demand of 50 MW, K_{WF} must be equal to 0.057. It can be seen that by increasing the pitch angle, the demand power is satisfied. For instance, the reference power of the first WECS becomes 0.87 pu. This value is lower than the maximum value, i.e., 0.99 pu. The difference between these values leads to acceleration of turbine and increase of pitch angle.

In the third case study, the performance of the WF under variation of wind speed is investigated. The profile of the wind speed for the first turbine is illustrated in Fig. 8. For modeling spatial distribution, it is assumed that wind needs 60s to travel from

Table 1 Comparison between the MPPT mode and constant power control mode in low wind speed condition

	Wind speed ($\frac{m}{s}$)	The MPPT mode ($K_{WF} = 0$)			The deloaded mode ($K_{WF} = 0.3$)		
		Output power (MW)	Rotational speed (pu)	Pitch angle (Deg)	Output power (MW)	Rotational speed (pu)	Pitch angle (Deg)
WECS 1	8	3.3	0.82	0	2.8	1	0
WECS 2	8.5	4	0.88	0	3.6	1.07	0
WECS 3	9	4.7	0.93	0	4	1.13	0
WECS 4	9.5	5.5	0.98	0	4.7	1.17	0
WECS 5	10	6.5	1.03	0	5.4	1.252	0.3
WECS 6	10.5	7.5	1.08	0	5.6	1.26	2.1
WF	–	30.5	–	–	25	–	–

Table 2 Comparison between the conventional and deloaded operations of turbines in high wind speed condition

	Wind speed ($\frac{m}{s}$)	Without reserve power ($K_{WF} = 0$)			The deloaded mode ($K_{WF} = 0.057$)		
		Output power (MW)	Rotational speed (pu)	Pitch angle (Deg)	Output power (MW)	Rotational speed (pu)	Pitch angle (Deg)
WECS 1	13	9.9	1.28	4.7	8.7	1.29	5.9
WECS 2	13.5	9.9	1.29	5.9	8.7	1.29	7
WECS 3	14	9.9	1.29	6.9	8.7	1.3	7.9
WECS 4	14.5	10	1.3	7.8	8.8	1.3	8.7
WECS 5	15	10	1.3	8.7	8.8	1.31	9.5
WECS 6	15.5	10	1.31	9.4	8.8	1.31	10.2
WF	–	56.7	–	–	50	–	–

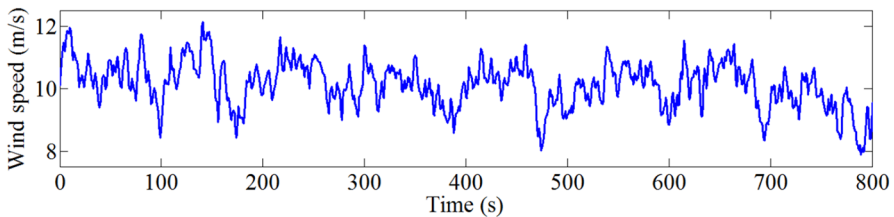


Fig. 8 Wind speed profile of WECS 1

one site to another one. Details about the wind speed characteristics of WECSs are depicted in Table 3.

The demand power of 30, 35, 25 and 40 MW, are required to be tracked during 0–200, 200–400, 400–600 and 600–800 s, respectively. The output power is illustrated in Fig. 9a. For quantifying the deviation to the demand power and also for evaluating

Table 3 Wind speed characteristics of WECSs

	Mean value ($\frac{m}{s}$)	Standard deviation ($\frac{m}{s}$)
WECS 1	10.14	0.72
WECS 2	10.06	0.72
WECS 3	10.03	0.72
WECS 4	9.96	0.66
WECS 5	9.94	0.65
WECS 6	9.9	0.65

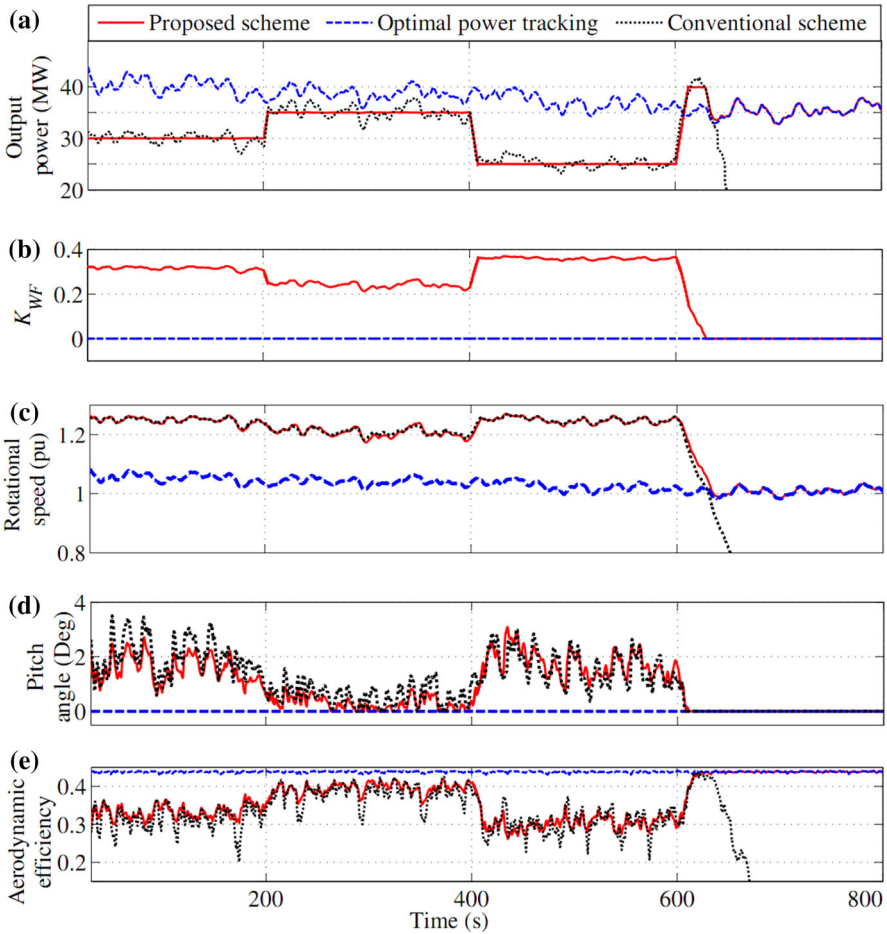


Fig. 9 Results of the third case study: **a** output power of WF, **b** variation of K_{WF} , **c** average value of the rotational speed of turbines, **d** average value of the pitch angle of turbines and **e** average value of the aerodynamic efficiency of turbines

Table 4 Standard deviation of output power of WF (MW)

Duration (s)	The MPPT method	The constant power control	
		The proposed scheme	The conventional scheme
0–200	1.94	0.07	1.02
200–400	1.12	0.03	1.08
400–600	1.38	0.06	0.82
600–800	1.2	1.7	Unstable

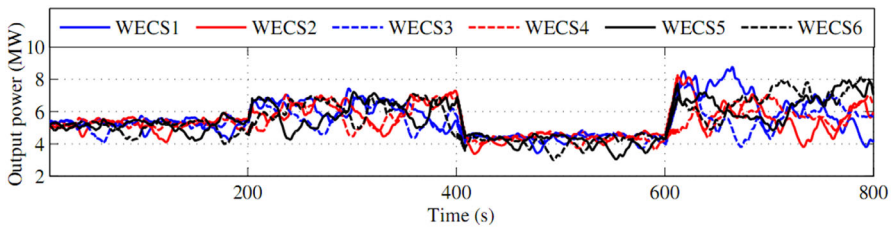


Fig. 10 Active power variation of individual WECSs (the proposed scheme)

the power fluctuations, the standard deviation of output power is calculated as follows:

$$\sigma_P = \sqrt{\frac{1}{N - 1} \sum_{i=1}^N (P - \bar{P})^2} \tag{11}$$

where N and \bar{P} are the sample number of data and the mean value of the active power, respectively. The standard deviation corresponds to the output power of the WF is listed in Table 4. The standard deviation of the proposed scheme is lower than that of the conventional scheme described in Sect. 3.1. Therefore, the proposed scheme tracks the reference power more precisely.

From 0 to 600 s, the proposed scheme operates in the deloaded state and the power demands are satisfied. When the demand is changed, K_{WF} is controlled by the supervisory controller and, as a result, the power reference for the local controller of the DFIGs is changed. As shown in Fig. 9b, the difference between the optimal and demand powers leads to an increase in K_{WF} and, therefore, the turbines accelerate and C_p decreases. When the rotational speed exceeds the ω_r^{max} , the pitch control system is activated to limit the speed of WECS. The mean value of the pitch angle of WECSs is given in Fig. 9d. It can be seen in Fig. 9 that as the power reserve increases, the rotational speed and the pitch angle increase too.

During 600–800s, the demand of 40MW is higher than the maximum available power of WF. Therefore, the instability occurs for the conventional scheme. In the proposed scheme, K_{WF} becomes zero and, according to Eq. 9, the maximum available power is extracted.

The active power of each DFIG is illustrated in Fig. 10. The power of WECSs is in allowable limits and excessive variations are not observed in their output power. The

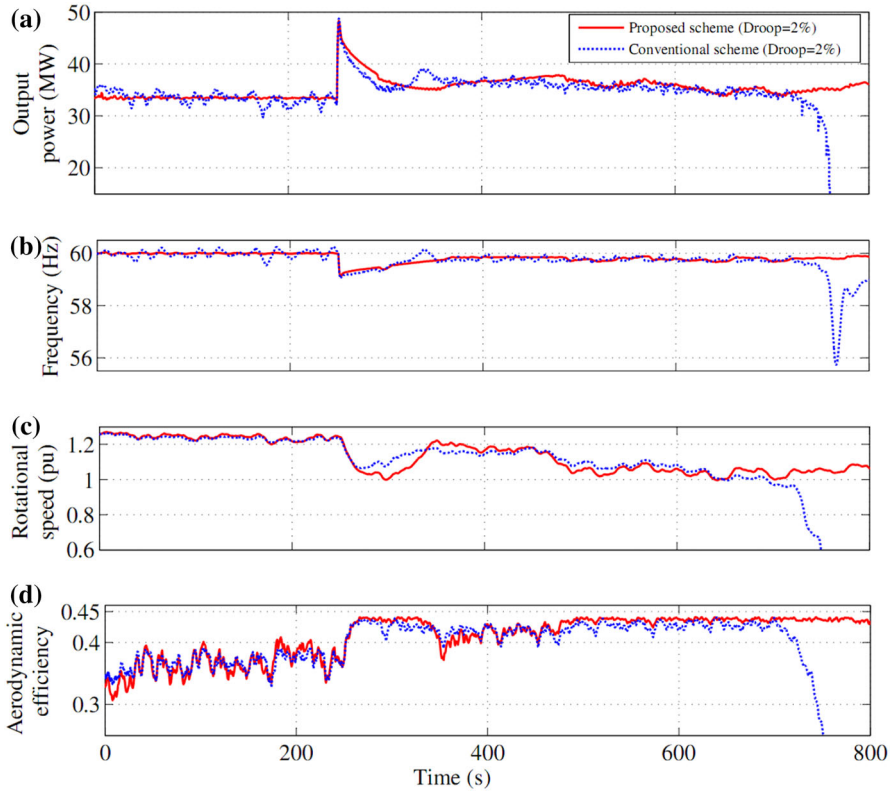


Fig. 11 Results of the fourth case study: **a** output power of WF, **b** frequency profile, **c** mean value of the rotational speed of turbines and **d** mean value of the aerodynamic efficiency of turbines

results show the capability of the proposed scheme to coordinate the WECs of the WF to produce a constant power.

5.3 Frequency control

In this section, comparisons are made between the performance of the proposed and conventional schemes from frequency control point of view. The conventional scheme is equipped with the inertial and the droop controls discussed in Sect. 3. The second scenario of the proposed scheme is used to enable the WF to participate in frequency control. At $t = 250$ s, the G4 is disconnected from the power system and, therefore, the frequency and the inertia of the power system decreases. This leads to loss of about 11% of the total generation. The profile of the wind speed is the same as the previous case study shown in Fig. 8.

In the fourth case study, the droop setting of 2% is applied for the conventional and proposed schemes. The output power of WF, profile of the frequency, the mean value of the rotational speed of turbines and the mean value of the aerodynamic efficiency of turbines are illustrated in Fig. 11. During 0–250 s, the WF operates in normal

Table 5 The results of case studies

	Scheme Operation mode Duration (s)	Conventional			Proposed		
		Deloaded	Inertial control	Droop control	Deloaded	Inertial control	Droop control
		0-250	250-260	260-800	0-250	250-260	260-800
Case 4	Droop value	2%	2%	2%	2%	2%	2%
	f (Hz)	59.98	59.21	59.6	60	59.28	59.75
	f_{min} (Hz)	59.55	59.05	55.74	59.95	59.12	59.3
	P_{WF} (MW)	33.5	43.5	Unstable	33.5	44.1	36.12
	$\sigma_{P_{WF}}$ (MW)	1.1	3.62	Unstable	0.13	3.37	0.96
	C_p	0.376	0.41	Unstable	0.375	0.41	0.432
Case 5	Droop value	4%	4%	4%	2%	2%	2%
	f (Hz)	59.98	59.21	59.72	60	59.28	59.75
	f_{min} (Hz)	59.55	59.05	59.19	59.95	59.12	59.3
	P_{WF} (MW)	33.5	43.5	34.13	33.5	44.1	36.12
	$\sigma_{P_{WF}}$ (MW)	1.1	3.62	1.05	0.13	3.37	0.96
	C_p	0.376	0.41	0.406	0.375	0.41	0.432
Case 6	Droop value	4%	4%	4%	2%	2%	2%
	f (Hz)	59.96	59.11	59.5	59.99	59.18	59.73
	f_{min} (Hz)	59.17	58.95	57.06	59.92	59.03	59.21
	P_{WF} (MW)	33.25	41.7	Unstable	33.7	43.2	34.5
	$\sigma_{P_{WF}}$ (MW)	1.89	3.4	Unstable	0.2	3.2	1.7
	C_p	0.363	0.39	Unstable	0.361	0.4	0.42

conditions, while during 250–260 s, the WF operates in the inertial control mode and during 260–800 s, it operates in the droop control mode.

In normal conditions, the WF operates in the deloaded state for reserving almost 15% of its generation. The mean value of the aerodynamic efficiency of turbines is shown in Fig. 11d and Table 5. From 0 to 250 s, C_p is lower than the maximum value, i.e., 0.44 for the given turbine, and therefore both schemes operate in the deloaded state. In the proposed scheme, the WF produces a constant power of 33.5 MW. Similar to the case of tracking a reference power, K_{WF} is controlled in such a way that the demand power is satisfied. As listed in Table 5, the standard deviations of output power for the proposed and the conventional schemes are 0.13 and 1.1 MW, respectively. Therefore, the proposed scheme mitigates the fluctuations of the output power. In the conventional scheme, the variation of the output power leads to oscillations in the frequency.

At $t=250$ s, the outage of the G4 causes a difference between load and generation and, therefore, the frequency deviates from the nominal value. Both schemes are equipped with the inertial control and once the frequency drops, the stored kinetic energy of the WECSs is fed into the grid. Consequently, the falling of frequency stops. During the inertial control, the injected output power is almost 44 MW which is higher than the maximum available power. This results in the reduction of the rotational speed of the WECSs. It should be noted that the investigation of the inertial response is not the focus of this paper.

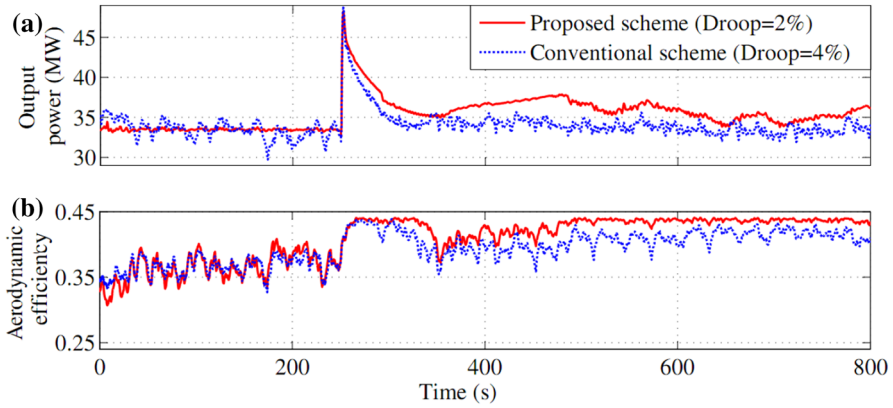


Fig. 12 Results of the fifth case study: **a** output power of the WF and **b** mean value of the aerodynamic efficiency of turbines

Sufficient generation reserve margin is available for participation in the primary frequency control. The mean value of the aerodynamic efficiency of the turbines increases over this period of time. As illustrated in Fig. 11d, the proposed scheme has a better performance in obtaining the maximum available power of WF.

At $t = 730$ s, the demand power becomes higher than the maximum available power and, therefore, the instability occurs in the conventional scheme. As illustrated in Fig. 11b and Table 5, due to the instability, the frequency becomes lower than 56 Hz. In an isolated power system, the allowable variation for the system frequency is between ± 1 Hz [36]. It is clear that in the conventional scheme, the deviation of the frequency exceeds the allowable limits.

Another case study is presented to verify the effect of droop value on stability and amount of extracted power of WF. In this case, the droop values of 2 and 4% are adjusted for the proposed and conventional schemes, respectively. The profile of wind speed is the same as the previous case study. Figure 12 illustrates the WF output power and the mean value of the aerodynamic efficiency of turbines. The performance of the controller in the deloaded state and inertial control mode are the same as the previous case study. However, during participation in primary frequency control, applying the higher value of droop for the conventional scheme results in producing the lower amount of the power and, consequently, the WF is stable. In this period of time, as illustrated in Table 5, the mean value of the aerodynamic efficiency of the turbines for the proposed and conventional schemes are 0.432 and 0.406, respectively. Since the WF aerodynamic efficiency for the proposed scheme is closer to the maximum value, the optimal frequency response is obtained.

In the sixth case study, the effect of variation of wind speed is investigated. The mean value of wind speed is equal to the previous case study. But, its standard deviation is considered to be $1.44 \frac{m}{s}$. The droop setting is the same as the previous case study. The variation of output power is shown in Fig. 13. As illustrated in Table 5, the standard deviation of output power increases during the deloaded operation. Furthermore, due

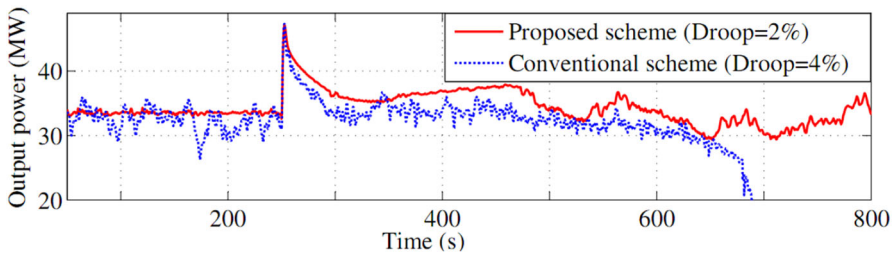


Fig. 13 Variation of the WF output power for the sixth case study

to excessive variation of wind speed, the conventional scheme with droop setting of 4% becomes unstable. In the proposed scheme, not only the stability is preserved, but also the WF aerodynamic efficiency increases during the droop control.

6 Discussion

This paper focuses on the primary frequency control support of DFIG-based WF. It has been explained that the wind turbine should have sufficient reserve power to be able to participate in the frequency control. It has been argued the conventional method of deloading a turbine is complicated and is dependent upon the turbine operating point and also increases the fluctuations of output power. In this paper, to resolve these issues, a simple supervisory controller has been proposed that coordinates all turbines in the WF.

It has been also discussed that the value of droop constant is very important for the stability of turbine. A low droop value may cause instability problem while a high value reduces the injected power of turbine. Although in other control schemes, variable droop strategy has been suggested for the stability purposes, implementing these schemes is not an easy task since they depend on the turbine operating point. The proposed scheme tries to coordinate turbines in the WF for preserving the stability even with a low droop value.

In the proposed scheme, the K_{Wf} signal needs to be transmitted from the supervisory controller to the wind turbine control system in real-time. However, the information of the maximum available power can be transmitted in quasi real-time from wind turbine control system to the supervisory controller. The proposed approach can easily be implemented using the present communication system of WF [32].

7 Conclusion

In this paper, a supervisory controller was proposed for the WF to coordinate the WECSs effectively. The scheme can be used in two different scenarios. In the first scenario, the capability of reference power tracking was investigated. In the second scenario, the capability of the WF to participate in the primary frequency control was investigated. It was shown that without any concern about the instability problem, a low value of droop can be set for the entire WF and, therefore, the optimal frequency

response of WF is achieved. The scheme does not depend on the WECSs operating point and therefore, its implementation is simple. Furthermore, it was shown that, the proposed scheme decreases the output power fluctuations of WF.

8 Appendix

8.1 WECS parameters

The parameters of the WECS are shown in Table 6.

Table 6 WECS parameters [35]

Rated Capacity (MW)	5
Rotor diameter (m)	126
Number of blades	3
Cut in wind speed (m/s)	3
Rated wind speed (m/s)	11.4
Cut out wind speed (m/s)	25
Turbine rated speed (rpm)	12.1
Generator rated speed (rpm)	1173.7
Rated generator torque (Nm)	43093.55
Maximum torque rate (N m/s)	15000
Generator inertia (Kg m^2)	534.114
Rotor inertia (Kg m^2)	3.8759×10^7
Maximum pitch angle (deg)	90
Minimum pitch angle (deg)	0
Maximum blade pitch rate (deg/s)	8

8.2 Hydro-power plant model

Figure 14a is the considered nonlinear model of hydro-turbine while Fig. 14b shows the considered PID-type governor [37].

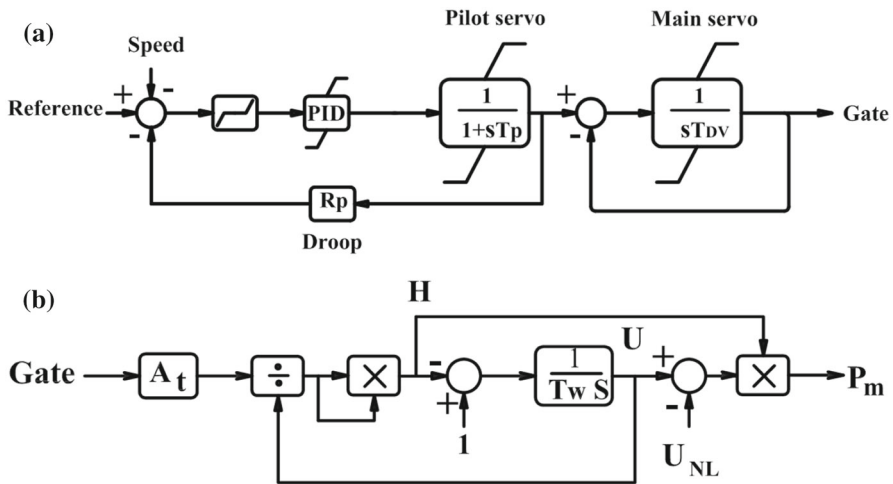


Fig. 14 Hydro-power plant model: **a** turbine model and **b** governor model

References

1. Shafiqullah, G., Oo, A.M.T., Ali, AShawkat, Wolfs, P.: Potential challenges of integrating large-scale wind energy into the power grid—a review. *Renew. Sustain. Energy Rev.* **20**, 306–321 (2013)
2. Pradhan, C., Bhende, C.: Adaptive deloading of stand-alone wind farm for primary frequency control. *Energy Syst.* **6**(1), 109–127 (2015)
3. Wang, Y., Meng, J., Zhang, X., Xu, L.: Control of PMSG-based wind turbines for system inertial response and power oscillation damping. *IEEE Trans. Sustain. Energy* **6**(2), 565–574 (2015)
4. Wilches-Bernal, F., Chow, J.H., Sanchez-Gasca, J.J.: A fundamental study of applying wind turbines for power system frequency control. *IEEE Trans. Power Syst.* **31**(2), 1496–1505 (2016)
5. Dreidy, M., Mokhlis, H., Mekhilef, S.: Inertia response and frequency control techniques for renewable energy sources: a review. *Renew. Sustain. Energy Rev.* **69**, 144–155 (2017)
6. Machowski, J., Bialek, J., Bumby, J.: *Power system dynamics: stability and control*. Wiley, New York (2011)
7. Liu, Y., Gracia, J.R., King, T.J., Liu, Y.: Frequency regulation and oscillation damping contributions of variable-speed wind generators in the US eastern interconnection (EI). *IEEE Trans. Sustain. Energy* **6**(3), 951–958 (2015)
8. De Rijcke, S., Tielens, P., Rawn, B., Van Hertem, D., Driesen, J.: Trading energy yield for frequency regulation: optimal control of kinetic energy in wind farms. *IEEE Trans. Power Syst.* **5**(30), 2469–2478 (2015)
9. Vidyanandan, K., Senroy, N.: Primary frequency regulation by deloaded wind turbines using variable droop. *IEEE Trans. Power Syst.* **28**(2), 837–846 (2013)
10. Liu, Y., Lin, J., Wu, Q., Zhou, X.: Frequency control of DFIG based wind power penetrated power systems using switching angle controller and AGC. *IEEE Trans. Power Syst.* **32**(2), 1553–1567 (2017)
11. Rose, S., Apt, J.: The cost of curtailing wind turbines for secondary frequency regulation capacity. *Energy Syst.* **5**(3), 407–422 (2014)
12. Hwang, M., Muljadi, E., Park, J.-W., Sorensen, P., Kang, Y.C.: Dynamic droop-based inertial control of a doubly-fed induction generator. *IEEE Trans. Sustain. Energy* **7**(3), 924–933 (2016)
13. Lee, J., Muljadi, E., Sorensen, P., Kang, Y.C.: Releasable kinetic energy-based inertial control of a DFIG wind power plant. *IEEE Trans. Sustain. Energy* **7**(1), 279–288 (2016)
14. Kayikci, M., Milanovic, J.V.: Dynamic contribution of DFIG-based wind plants to system frequency disturbances. *IEEE Trans. Power Syst.* **24**(2), 859–867 (2009)
15. Kang, M., Kim, K., Muljadi, E., Park, J.-W., Kang, Y.C.: Frequency control support of a doubly-fed induction generator based on the torque limit. *IEEE Trans. Power Syst.* **31**(6), 4575–4583 (2016)

16. Ye, H., Pei, W., Qi, Z.: Analytical modeling of inertial and droop responses from a wind farm for short-term frequency regulation in power systems. *IEEE Trans. Power Syst.* **31**(5), 3414–3423 (2016)
17. Zhao, J., Lyu, X., Fu, Y., Hu, X., Li, F.: Coordinated microgrid frequency regulation based on DFIG variable coefficient using virtual inertia and primary frequency control. *IEEE Trans. Energy Convers.* **31**(3), 833–845 (2016)
18. Lin, J., Sun, Y., Song, Y., Gao, W., Sorensen, P.: Wind power fluctuation smoothing controller based on risk assessment of grid frequency deviation in an isolated system. *IEEE Trans. Sustain. Energy* **4**(2), 379–392 (2013)
19. Xu, J., Liao, S., Sun, Y., Ma, X.-Y., Gao, W., Li, X., Gu, J., Dong, J., Zhou, M.: An isolated industrial power system driven by wind-coal power for aluminum productions: a case study of frequency control. *IEEE Trans. Power Syst.* **30**(1), 471–483 (2015)
20. Ghani Varzaneh, S., Gharehpetian, G., Abedi, M.: Output power smoothing of variable speed wind farms using rotor-inertia. *Electr. Power Syst. Res.* **116**, 208–217 (2014)
21. Saejia, M., Ngamroo, I.: Alleviation of power fluctuation in interconnected power systems with wind farm by SMES with optimal coil size. *IEEE Trans. Appl. Supercond.* **22**(3), 5701504–5701504 (2012)
22. Howlader, A.M., Senjyu, T., Saber, A.Y.: An integrated power smoothing control for a grid-interactive wind farm considering wake effects. *IEEE Syst. J.* **9**(3), 954–965 (2015)
23. Crdenas, R., Pea, R., Alepez, S., Asher, G.: Overview of control systems for the operation of DFIGs in wind energy applications. *IEEE Trans. Industr. Electron.* **60**(7), 2776–2798 (2013)
24. Ghoudelbour, S., Dib, D., Omeiri, A.: Decoupled control of active and reactive power of a wind turbine based on DFIG and matrix converter. *Energy Syst.* **7**(3), 483–497 (2015)
25. Pena, R., Clare, J., Asher, G.: Doubly fed induction generator using back-to-back PWM converters and its application to variable-speed wind-energy generation. *IEE Proc. Electr. Power Appl.* **3**, 231–241 (1996)
26. Tapia, A., Tapia, G., Ostolaza, J.X., Saenz, J.R.: Modeling and control of a wind turbine driven doubly fed induction generator. *IEEE Trans. Energy Convers.* **18**(2), 194–204 (2003)
27. Ghani Varzaneh, S., Rastegar, H., Gharehpetian, G.: A new three-mode maximum power point tracking algorithm for doubly fed induction generator based wind energy conversion system. *Electric Power Compon. Syst.* **42**(1), 45–59 (2014)
28. Fouad, K., Boulouiha, H.M., Allali, A., Taibi, A., Denai, M.: Multivariable control of a grid-connected wind energy conversion system with power quality enhancement. *Energy Syst.* **9**(1), 25–57 (2016)
29. Tan, Y., Meegahaolla, L., Muttaqi, K.M.: A suboptimal power-point-tracking-based primary frequency response strategy for DFIGs in hybrid remote area power supply systems. *IEEE Trans. Energy Convers.* **31**(1), 93–105 (2016)
30. Van de Vyver, J., De Kooning, J.D., Meersman, B., Vandeveld, L., Vandoorn, T.L.: Droop control as an alternative inertial response strategy for the synthetic inertia on wind turbines. *IEEE Trans. Power Syst.* **31**(2), 1129–1138 (2016)
31. Wang, Y., Delille, G., Bayem, H., Guillaud, X., Francois, B.: High wind power penetration in isolated power systems assessment of wind inertial and primary frequency responses. *IEEE Trans. Power Syst.* **28**(3), 2412–2420 (2013)
32. Gao, Z., Geng, J., Zhang, K., Dai, Z., Bai, X., Peng, M., Wang, Y.: Wind power dispatch supporting technologies and its implementation. *IEEE Trans. Smart Grid* **4**(3), 1684–1691 (2013)
33. Keung, P.-K., Li, P., Banakar, H., Ooi, B.T.: Kinetic energy of wind-turbine generators for system frequency support. *IEEE Trans. Power Syst.* **24**(1), 279–287 (2009)
34. Ali, M., Ilie, I.-S., Milanovic, J.V., Chicco, G.: Wind farm model aggregation using probabilistic clustering. *IEEE Trans. Power Syst.* **28**(1), 309–316 (2013)
35. Jonkman, J., Butterfield, S., Musial, W., Scott, G.: Definition of a 5-MW reference wind turbine for offshore system development. National Renewable Energy Laboratory, Golden, CO, Technical Report No. NREL/TP-500-38060 (2009)
36. Almeida, P.R., Soares, F., Lopes, J.P.: Electric vehicles contribution for frequency control with inertial emulation. *Electr. Power Syst. Res.* **127**, 141–150 (2015)
37. Kundur, P.: Power system stability and control. Tata McGraw-Hill Education, Chennai (1994)